

ARMY RESEARCH LABORATORY



Ku-Band Radio Frequency Microelectromechanical System Enabled Electronically Scanned Antenna

by Ronald G. Polcawich, Daniel Judy, Jeffrey S. Pulskamp, and Steve Weiss

ARL-TR-4280

October 2007

NOTICES

Disclaimers

The findings in this report are not to be construed as an official Department of the Army position unless so designated by other authorized documents.

Citation of manufacturer's or trade names does not constitute an official endorsement or approval of the use thereof.

Destroy this report when it is no longer needed. Do not return it to the originator.

Army Research Laboratory

Adelphi, MD 20783-1197

ARL-TR-4280

October 2007

Ku-Band Radio Frequency Microelectromechanical System Enabled Electronically Scanned Antenna

Ronald G. Polcawich, Daniel Judy, Jeffrey S. Pulskamp, and Steve Weiss

*U.S. Army Research Laboratory
Sensors and Electron Devices Directorate*

REPORT DOCUMENTATION PAGE

*Form Approved
OMB No. 0704-0188*

Public reporting burden for this collection of information is estimated to average 1 hour per response, including the time for reviewing instructions, searching existing data sources, gathering and maintaining the data needed, and completing and reviewing the collection information. Send comments regarding this burden estimate or any other aspect of this collection of information, including suggestions for reducing the burden, to Department of Defense, Washington Headquarters Services, Directorate for Information Operations and Reports (0704-0188), 1215 Jefferson Davis Highway, Suite 1204, Arlington, VA 22202-4302. Respondents should be aware that notwithstanding any other provision of law, no person shall be subject to any penalty for failing to comply with a collection of information if it does not display a currently valid OMB control number.

PLEASE DO NOT RETURN YOUR FORM TO THE ABOVE ADDRESS.

1. REPORT DATE (DD-MM-YYYY)	2. REPORT TYPE		3. DATES COVERED (From - To)		
October 2007	Summary		May 2005 to April 2006		
4. TITLE AND SUBTITLE Ku-Band Radio Frequency Microelectromechanical System Enabled Electronically Scanned Antenna			5a. CONTRACT NUMBER		
			5b. GRANT NUMBER		
			5c. PROGRAM ELEMENT NUMBER		
6. AUTHOR(S) Ronald G. Polcawich, Daniel Judy, Jeffrey S. Pulskamp, and Steve Weiss			5d. PROJECT NUMBER		
			5e. TASK NUMBER		
			5f. WORK UNIT NUMBER		
7. PERFORMING ORGANIZATION NAME(S) AND ADDRESS(ES) U.S. Army Research Laboratory ATTN: AMSRD-ARL-SE-RL 2800 Powder Mill Road Adelphi, MD 20783-1197			8. PERFORMING ORGANIZATION REPORT NUMBER		
			ARL-TR-4280		
9. SPONSORING/MONITORING AGENCY NAME(S) AND ADDRESS(ES) U.S. Army Research Laboratory 2800 Powder Mill Road Adelphi, MD 20783-1197			10. SPONSOR/MONITOR'S ACRONYM(S)		
			11. SPONSOR/MONITOR'S REPORT NUMBER(S)		
			ARL-TR-4280		
12. DISTRIBUTION/AVAILABILITY STATEMENT Approved for public release; distribution unlimited.					
13. SUPPLEMENTARY NOTES					
14. ABSTRACT The Army Research Laboratory (ARL) has designed, fabricated, and measured an eight element Ku-band radio frequency (RF) microelectromechanical system (MEMS) based electronically scanned antenna (ESA). This ESA is comprised of eight patch antennas with each patch individually fed by separate phase shifters. The reflection phase shifters use ARL's patent pending MEMS ohmic shunt switch. The ohmic shunt switch performance characteristics include insertion loss less than 0.3 decibel (dB) and isolation greater than 20 dB from direct current (DC) to 40 gigahertz (GHz). The 17 GHz phase shifters have an average insertion loss of 2.5 dB and a return loss greater than 20 dB. The effort resulted in successful beam steering using RF MEMS phase shifters. The work represents ARL's continuing effort in low-cost electronically scanned antennas in support of the Future Force.					
15. SUBJECT TERMS MEMS; Phase Shifter; Antenna; Electronically Scanned Array, ESA, Electrostatic					
16. SECURITY CLASSIFICATION OF:			17. LIMITATION OF ABSTRACT SAR	18. NUMBER OF PAGES 20	19a. NAME OF RESPONSIBLE PERSON Ronald G. Polcawich
a. REPORT U	b. ABSTRACT U	c. THIS PAGE U			19b. TELEPHONE NUMBER (Include area code) (301) 394-1275

Contents

List of Figures	iv
List of Tables	iv
Acknowledgments	v
1. Introduction	1
2. Experimental Procedure	1
3. Results and Discussion	5
3.1 Electrostatic Shunt Switch.....	5
3.2 MEMS Phase Shifter	6
3.3 Antenna (17 GHz 1x8 Linear Patch Array).....	7
4. Conclusion	9
References	10
Acronyms and Abbreviations	11
Distribution List	12

List of Figures

Figure 1. Reflection type MEMS phase shifter	2
Figure 2. RF MEMS phase shifter package	3
Figure 3. Patch antenna array.....	3
Figure 4. Phase shifter control panel consisting of rotary switches for each of the phase shifters.	4
Figure 5. ESA held in position.....	4
Figure 6. Measured S parameters of the ohmic shunt electrostatic switch in the (a) off state, and (b) on state.....	5
Figure 7. 3-bit phase shifters.....	6
Figure 8. Measured S parameter of the 2-bit 17GHz phase shifter (16–20 GHz).	7
Figure 9. EMPIcasso simulations.....	8
Figure 10. MEMS ESA reconfigured plots.....	8

List of Tables

Table 1. Summary of electrostatic shunt switch performance.....	5
Table 2. The 17 and 35 GHz phase shifter performance summary.	6

Acknowledgments

The authors would like to thank Richard Piekarz, Derwin Washington, and John Conrad for their assistance in the fabrication of the microelectromechanical system (MEMS) devices and Robert Dahlstrom for his assistance in measuring the antenna performance. Additionally, the authors appreciate all the hard work by Dennis Martin, Khamsouk Kingkeo, and Andrew Bayba on the phase shifter package design and assembly. Lastly, Dr. Madan Dubey and Edward Viveiros are acknowledged for the many discussions on MEMS device integration with radio frequency (RF) systems.

INTENTIONALLY LEFT BLANK.

1. Introduction

Radio frequency (RF) microelectromechanical system (MEMS) research has been ongoing for well over a decade. This research area has been strongly focused on developing robust, reliable MEMS switches and phase shifters for cell phone, electronic scanning antenna, and radar applications. Previous and existing research into RF MEMS switches and phase shifters has been focused primarily on electrostatic actuation with a few efforts in other actuation mechanisms such as thermal, piezoelectric, and magnetic (1). The relative simplicity and ease of integration of the electrostatic actuation mechanism is one of the key reasons for its larger research base. The most advanced switch programs include Radant's electrostatic ohmic series switch; Lincoln Laboratories electrostatic capacitive shunt switch; MEMtronics electrostatic capacitive shunt switch; and Raytheon's electrostatic capacitive shunt switch. Each of these research efforts has demonstrated excellent performance for RF switches including insertion loss, isolation, and reliability. To date, Rockwell and Raytheon have demonstrated some of the best performing phase shifters (2–6). With this background, the goal of our research program has been to demonstrate an electronically scanned antenna (ESA) with RF MEMS phase shifters. This demonstration platform could then be used to evaluate MEMS phase shifter performance within an ESA.

2. Experimental Procedure

MEMS switches and phase shifters were fabricated on high resistivity (>10 kOhm) silicon substrates at the Army Research Laboratory (ARL) specialty electronics cleanroom. The patent pending fabrication process will not be discussed in this section but is referenced in the patent disclosure filed by Pulskamp, et al. (7). Wafers completed fabrication and underwent switch performance testing on a Cascade wafer probe station.

For a MEMS phase shifter, a reflection phase shifter architecture was chosen to best use the performance of the switch and shrink the overall dimensions of the phase shifter (8–10). The MEMS phase shifter uses a co-planar waveguide (CPW) coupled line directional coupler, and two delay lines with shunt switches located at the appropriate location for the desired phase states (figure 1). The RF input and output were located at the bottom left and right; the switches were operated in pairs from right to left for the 0° , 90° , and 180° phase states, respectively. The 270° phase state uses the CPW short at the end of the transmission line, located at the top of the image. If the delay along the two delay lines is equal, the microwave energy reflected from the closed switch pair (or shorted line) add in phase at the output of the coupler with a phase shift equal to twice the delay associated with length of the delay line.

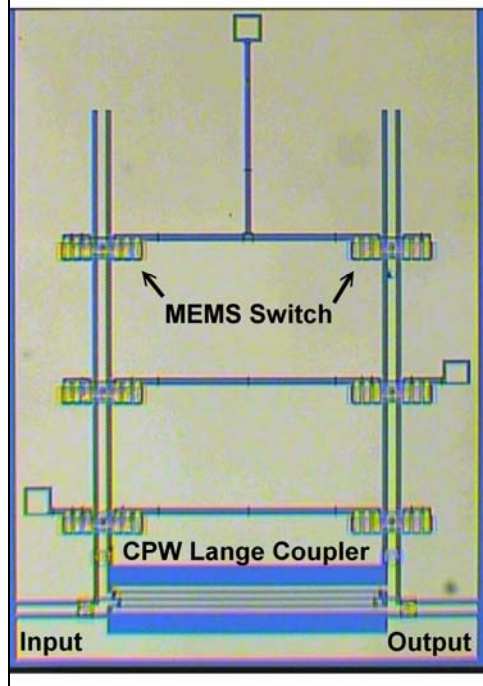


Figure 1. Reflection type MEMS phase shifter.

NOTE: Completed 2-bit reflection type MEMS phase shifter die ($2.75\text{mm} \times 4\text{mm}$) with 6 electrostatic shunt switches and integrated Lange coupler.

After initial wafers with MEMS phase shifters were successfully tested, additional wafers were fabricated with the intent of separating individual die prior to the final device release. For these wafers, completed phase shifter die with dimensions of 4 by 2.75 millimeter (mm) (17 gigahertz (GHz) design) were diced and separated from the wafer and prepared for device inspection. Completed die were placed into a silicon carrier wafer with recessed cavities for the die. The carrier wafer was placed onto a support chuck within a Cascade wafer probe station. Each die were tested for functionality of all phase states.

Experimental testing of switches and phase shifters was completed with a HP 8510 network analyzer in conjunction with two RF probes used with the Cascade wafer probe station. Switch testing consisted of gathering S-parameter measurements from 45 megahertz (MHz) to 40 GHz in both the open and closed states. For the phase shifters, S-parameters were collected from 16 to 18 GHz of each of the available phase states of the phase shifter (i.e., four for the 2-bit phase shifters and eight for the 3-bit phase shifters). Following RF performance evaluation, functional phase shifters were marked and selected for package and assembly.

The phase shifter package, seen in figure 2, consists of a cavity for the MEMS die and connectors for both direct current (DC) and RF contacts. The DC bias pads of each of the MEMS switches are wirebonded to one of the eight contact pins. The RF pathway consists of GPPO connectors on the outside of the package; transition to sections of microstrip (8.4 mm long); a J-Micro microstrip to CPW transition; and the MEMS phase shifter die placed between and wirebonded to the two J-Micro connectors.



Figure 2. RF MEMS phase shifter package.

NOTE: Package includes eight pins for DC bias contacts, microstrip sections, J-Micro microstrip to CPW transitions, and GPPO connections.

Following assembly, the connectorized MEMS phase shifters undergo another round of RF testing to verify each of the available phase states were still operable. This additional testing allows for selection of the eight phase shifters that have similar performance including phase state, return loss, and insertion loss. After the selection process, the packages were ready to populate the patch antenna array. The patch antenna array in figure 3 consists of an RF input port, sections of microstrip with splitters to each of the eight phase shifters, and each of the eight slot fed patch antennas.

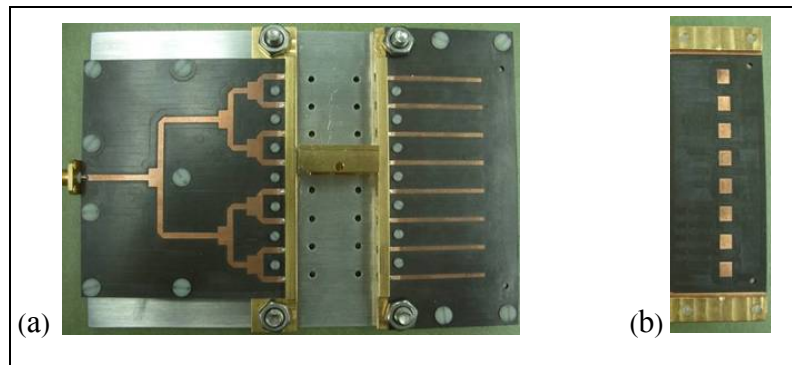


Figure 3. Patch antenna array.

NOTE: (a) Back view showing linear patch antenna array with microstrip transmission lines on a duroid substrate, a section for the eight phase shifters, and (b) front view showing eight slot fed patch antennas.

The assembled MEMS ESA was prepared for testing, by completing the wiring of each of the DC control lines to the phase shifter control panel, as shown in figure 4. The control panel has rotary switches to choose one of the four available phase states, along with resistors and capacitors soldered to each of the switch locations. This reduces any transient signals during the phase state selection process. The input to the phase shifter control panel consisted of two wires that were connected to a DC power supply.

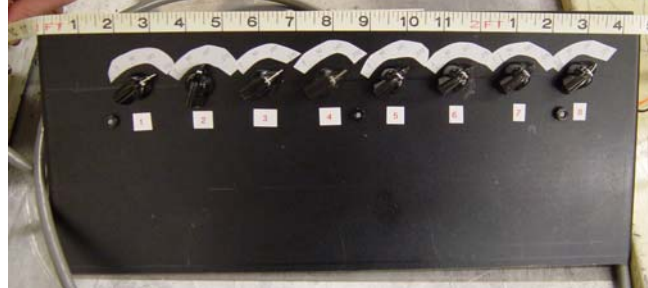


Figure 4. Phase shifter control panel consisting of rotary switches for each of the phase shifters.

Testing of the MEMS ESA occurred in an anechoic chamber at ARL October 2005 and again April 2006. All testing was performed with the MEMS ESA in receive mode with the transmitted 17 GHz continuous wave (CW) signal coming from a specified waveguide horn antenna operating from 15 to 22 GHz. Figure 5 shows the ESA held in position using a clamping circuit board holder and tape. The horn antenna was supplied with RF energy from a Wiltron 68347B signal generator, while the MEMS ESA was positioned approximately 50 ft from the horn. The ESA was attached to a block of foam attached to a rotating stage platform. The output from the ESA was connected to the mixer driven at 1.5 milliampere (mA) and measured with a bandwidth of 6 on the detector. The output from the detector, phase locked at 17 GHz, and the rotating stage controller was captured via a Labview generated program and stored at 1° increments from -90° to +90°.

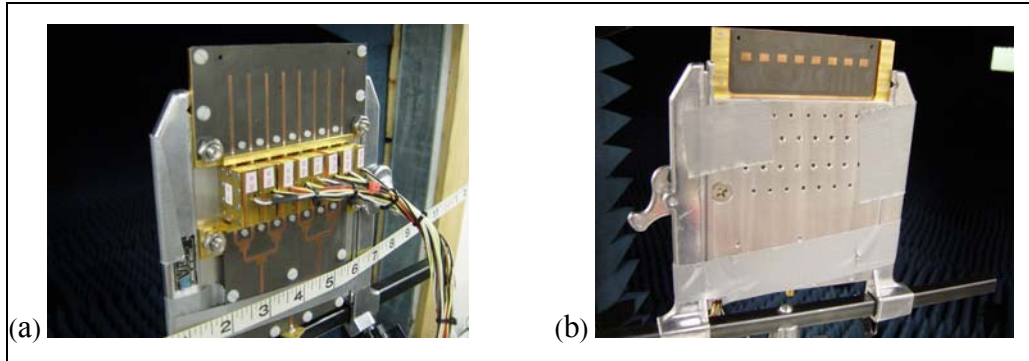


Figure 5. ESA held in position.

NOTE: (a) Shows the backside view mounted and fixtured MEMS ESA with clamping circuit board holder and tape keeping the antenna position fixed, and (b) front view of the MEMS ESA.

In order to establish the absolute gain of the MEMS ESA, a standard gain horn antenna was used to receive the transmit signal. The standard gain horn was measured with the same parameters as the MEMS ESA except it was scanned from -10° to $+10^\circ$.

3. Results and Discussion

3.1 Electrostatic Shunt Switch

ARL has developed a robust fabrication process and a sound mechanical and microwave design for a MEMS RF switch. The program goal of a low-loss, low-power consumption RF MEMS switch was successfully achieved in 2004. The patent pending ohmic shunt switch has a nominal operating voltage of 40 to 50V, is very broadband, and capable of operating from DC to at least 40 GHz with an insertion loss < 0.3 decibel (dB) and isolation > 20 dB, as illustrated in figure 6. A summary of the performance characteristics is listed in table 1 including values for 17 and 35 GHz.

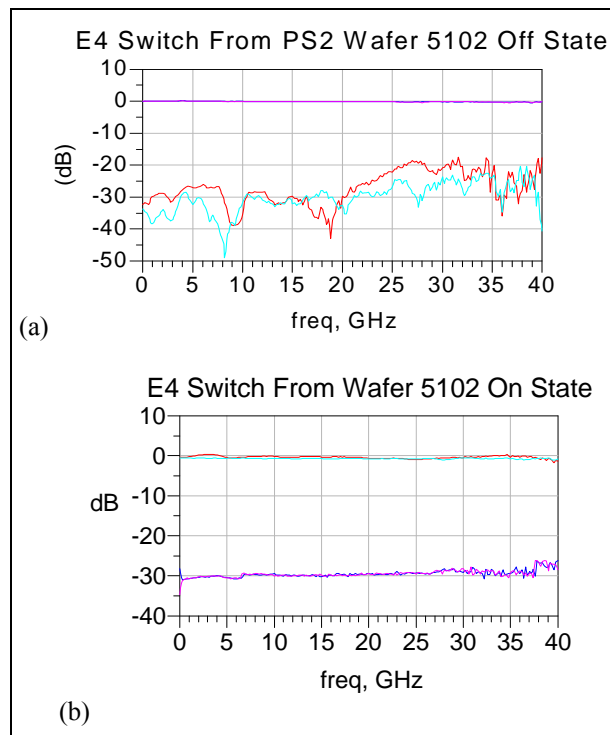


Figure 6. Measured S parameters of the ohmic shunt electrostatic switch in the (a) off state, and (b) on state.

Table 1. Summary of electrostatic shunt switch performance.

dB	45 MHz	Ku-band (17GHz)	Ka-band (35 GHz)
Insertion Loss	<.1	0.18	0.31
Return Loss	32	30	24
Isolation	32	30	29

3.2 MEMS Phase Shifter

In addition to the 2-bit phase shifter at 17 GHz, figure 7 shows the 3-bit phase shifters at 17 and 35 GHz were designed, fabricated, and tested. The performance characteristics of all of the phase shifters are summarized in table 2, and the S parameter plots for the 2-bit 17 GHz phase are shown in figure 8. Both 17 GHz designs have an average insertion loss of 2.5 dB, while the 35 GHz design has an average loss of 3.3 dB possibly a problem with the coupler design. The return loss for each of the phase shifters was greater than 20dB and the phase error is $\pm 5^\circ$ on average for both 17 GHz designs and increases to nearly 10° for the 35 GHz design.

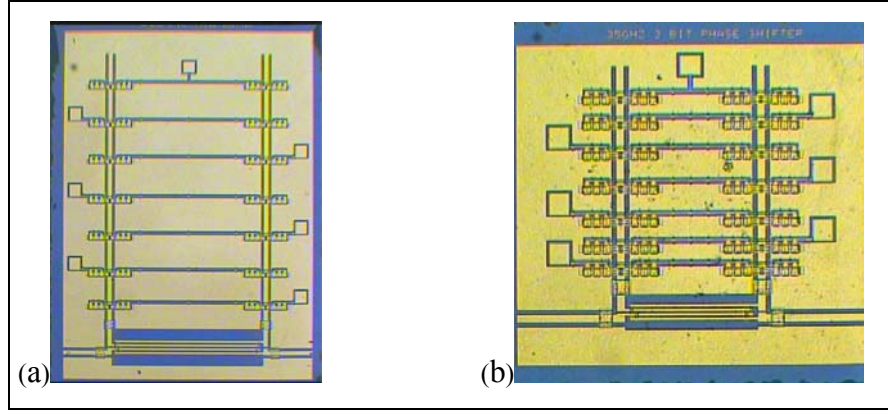


Figure 7. 3-bit phase shifters.

NOTE: (a) The 3-bit 17 GHz and 3 bit 35 GHz, and (b) designs are shown with the 17 GHz design having a footprint of $2.8 \times 4\text{mm}$ while the 35 GHz design has a footprint of $2.2 \times 2.1\text{mm}$.

Table 2. The 17 and 35 GHz phase shifter performance summary.

Degrees	Phase States							
	0	45	90	135	180	225	270	315
2 bit 17 GHz								
Insertion Loss (dB)	2.1	N/A	2.3	N/A	2.7	N/A	3.1	N/A
Phase Error ($^\circ$)	0	N/A	-6	N/A	2	N/A	-5	N/A
3 bit 17 GHz								
Insertion Loss (dB)	2.6	1.9	2.0	2.3	2.4	2.8	3.0	3.7
Phase Error ($^\circ$)	0	-9	-5	-4	-3	1	0	-3
3 bit 35 GHz								
Insertion Loss (dB)	2.5	2.1	2.1	2.4	3.3	4.3	5.5	4.3
Phase Error ($^\circ$)	0	-12	-8	5	-16	14	13	10

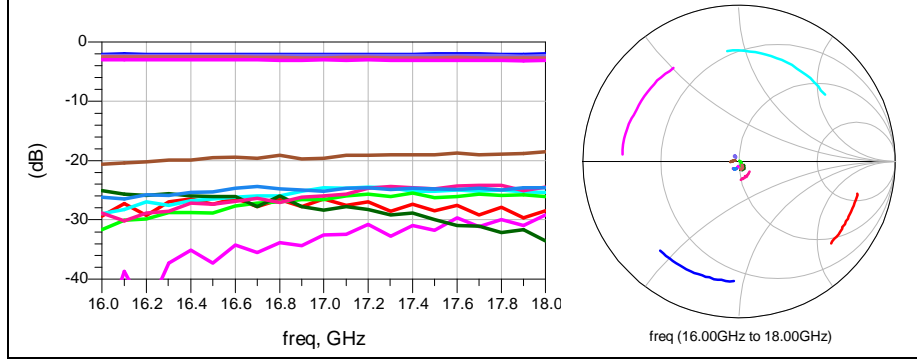


Figure 8. Measured S parameter of the 2-bit 17GHz phase shifter (16–20 GHz).

NOTE: The 0° state is the red trace, the 90° state is the blue trace, the 180° state is the magenta trace, and the 270° state is the cyan trace.

3.3 Antenna (17 GHz 1x8 Linear Patch Array)

Using the 2-bit phase shifters, the linear 1×8 patch antenna array was capable of detecting up to five different collective phase states. The states were labeled with the phase shift ($\Delta\phi$) between phase shifters as the indicator for the possible states ($0, 90, -90, 180, -180$). Values were recorded for a $\Delta\phi$ of zero with all phase shifters at 0° (shortest path length of the phase shifter) and with all phase shifters at 270° (i.e., longest path with all MEMS switches off, open).

The MEMS ESA performed well with each of the five possible beam positions detected. The single lobed beam was shifted approximately 23° for a $\Delta\phi$ of ± 90 . While, the receiving beam pattern exhibited dual lobes near 53° for a $\Delta\phi$ of ± 180 . In addition, each measured result was close to the theoretical predictions based on EMPiCASSO simulations as shown in figure 9.

Using the performance of the standard gain horn, figure 10 shows the MEMS ESA plots reconfigured with reference to a perfect isotropic radiator. The maximum gain displayed by the MEMS ESA was 1.22 dB_i at a $\Delta\phi$ of 0° , 1.84 dB_i at a $\Delta\phi$ of 90° , and -1.6 dB_i at a $\Delta\phi$ of 180° . The side lobes were depressed -6.4 dB for a $\Delta\phi$ of 0° and -7.3 dB for a $\Delta\phi$ of 90° .

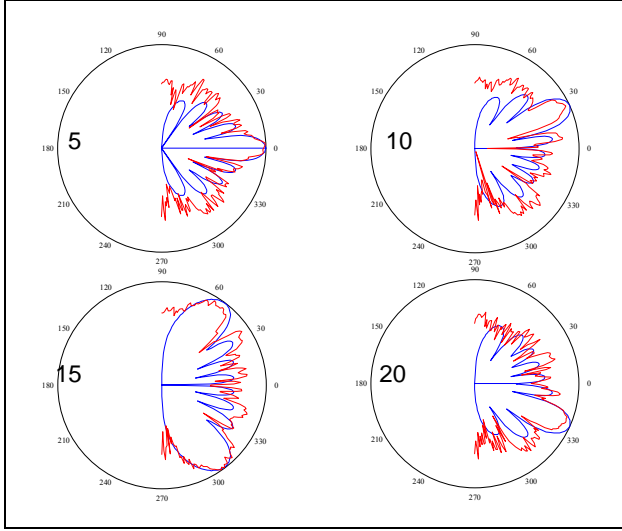


Figure 9. EMPiCasso simulations.

NOTE: Measured array patterns (red) with predictions from
EMPiCasso simulations (blue): (state 0) $\Delta\phi$ of 0° ,
(state 1) $\Delta\phi$ of 90° , (state 2) $\Delta\phi$ of 180° , (state 3) $\Delta\phi$ of -90° .

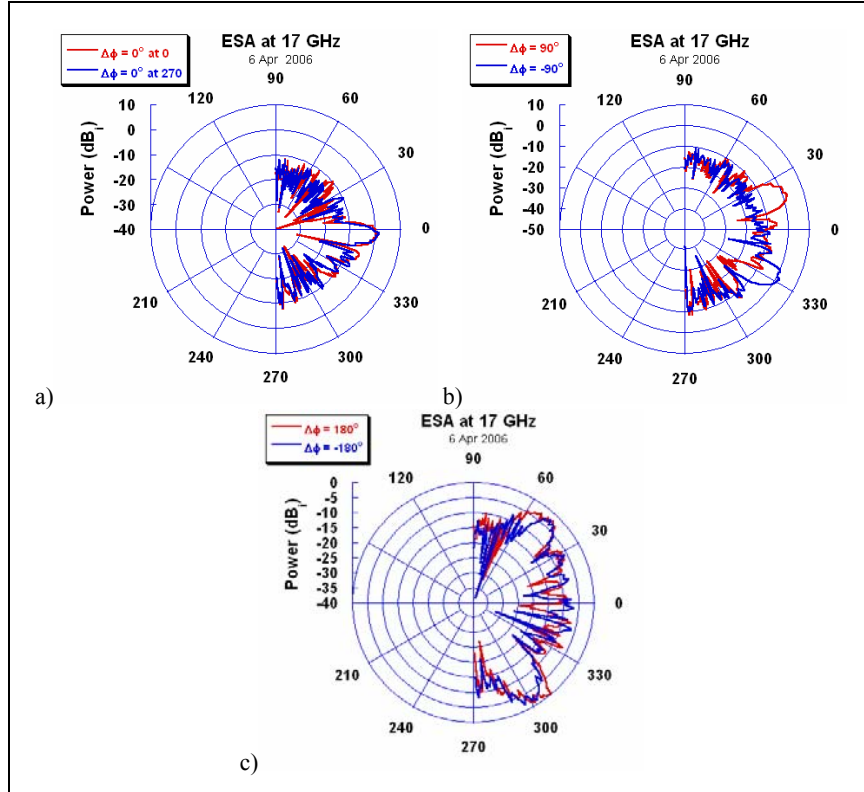


Figure 10. MEMS ESA reconfigured plots.

NOTE: MEMS ESA performance normalized with measurements from a standard gain horn antenna, (a) $\Delta\phi$ of 0° , (b) $\Delta\phi$ of $\pm 90^\circ$, and (c) $\Delta\phi$ of $\pm 180^\circ$.

4. Conclusion

Using a novel electrostatic ohmic shunt switch, engineers at ARL have demonstrated low-loss digital phase shifters at 17 GHz and 35 GHz with average loss of about 2.5 dB and 3.3 dB, respectively. The phase shifters were packaged and placed into a 1×8 linear patch array at 17 GHz. The patch array, representing a MEMS enabled ESA, functioned well exhibiting beam steering for each of the five available beam positions (0° , 25° , -25° , and $\pm 55^\circ$) using eight 2-bit MEMS phase shifters. The maximum gain displayed by the MEMS ESA was at a $\Delta\varphi$ of 0° , at a $\Delta\varphi$ of 90° , and at a $\Delta\varphi$ of 180° .

References

1. Rebeiz, G. *RF MEMS Theory Design, and Technology*; John Wiley and Sons, Inc., Ch. 5 and 9, 2003.
2. Kim, M.; Hacker, J.B.; Mihailovich, R.E.; DeNatale, J.F. A DC to 40 GHz four-bit RF MEMS True-Time Delay Network. *IEEE Microwave Wireless Comp. Lett.* **Feb 2001**, *11* (2), 56–8.
3. Hacker, J.B.; Mihailovich, R.E.; Kim, M.; DeNatale, J.F. A Ka-band three-bit RF MEMS True-Time Delay Network. *IEEE Trans. Microwave Theory Tech.* **Jan 2003**, *51* (1), 305-8.
4. Tan, G.L.; Mihailovich, R.E.; Hacker, J.B.; DeNatale, J.F.; Rebeiz, G.M. A Very-Low-Loss 2-bit X-band RF MEMS Phase Shifter. *IEEE International Microwave Symp Digest*, Seattle, WA, June 2002.
5. Tan, G.L.; Mihailovich, R.E.; Hacker, J.B.; DeNatale, J.F.; Rebeiz, G.M. Low-Loss 2- and 4-bit TTD MEMS Phase Shifters Based on SP4T Switches. *IEEE Trans. Microwave Theory Tech.* **Jan 2003**, *51* (1), 297–304.
6. Pillans, B.; Eshelman, S.; Malczewski, A.; Ehmke, J.; Goldsmith, C. Ka-band RF MEMS Phase Shifters. *IEEE Microwave Guided Wave Lett.* **Dec 1999**, *9* (12), 520-2.
7. Pulskamp, J.; Judy, D.; Polcawich, R. Electrostatic Ohmic Shunt Switch. ARL patent disclosure, 05–69.
8. Rebeiz, G. *RF MEMS Theory Design, and Technology*; John Wiley and Sons, Inc., Ch. 9, 2003.
9. Kim, H-T; Park, J.H.; Yim, J.; Kim, Y-K; Kwon, Y. A compact V-band 2-bit Reflection-Type MEMS Phase Shifter. *IEEE Microwave and Wireless Comp. Lett.* **Sept 2002**, *12* (9).
10. Malczewski, A.; Eshelman, S.; Pillans, B.G.; Ehmke, J.; Goldsmith, C.L. X-band RF MEMS Phase Shifters for Phased Array Applications. *IEEE Microwave Guided Lett.* **Dec 1999**, *9* (12).

Acronyms and Abbreviations

ARL	U.S. Army Research Laboratory
CPW	coplanar waveguide
CW	continuous wave
dB	decibel
DC	direct current
ESA	electronically scanned antenna
GHz	gigahertz
mA	millampere
MEMS	microelectromechanical system
MHz	megahertz
mm	millimeter
RF	radio frequency

Distribution List

	<u>NO.</u> <u>COPIES ORGANIZATION</u>	<u>NO.</u> <u>COPIES ORGANIZATION</u>
1 elec	ADMNSTR DEFNS TECHL INFO CTR ATTN DTIC OCP (ELECTRONIC COPY) 8725 JOHN J KINGMAN RD STE 0944 FT BELVOIR VA 22060-6218	1 HC COMMANDER US ARMY RDECOM ATTN AMSRD AMR W C MCCORKLE 5400 FOWLER RD REDSTONE ARSENAL AL 35898-5000
1 HC	DARPA ATTN IXO S WELBY 3701 N FAIRFAX DR ARLINGTON VA 22203-1714	1 HC US ARMY RSRCH LAB ATTN AMSRD ARL CI OK TP TECHL LIB T LANDFRIED BLDG 4600 APG MD 21005-5066
1 HC	OFC OF THE SECY OF DEFNS ATTN ODDRE (R&AT) THE PENTAGON WASHINGTON DC 20301-3080	1 HC US GOVERNMENT PRINT OFF DEPOSITORY RECEIVING SECTION ATTN MAIL STOP IDAD J TATE 732 NORTH CAPITOL ST NW WASHINGTON DC 20402
1 HC	US ARMY RSRCH DEV & ENGRG CMND ARMAMENT RSRCH DEV & ENGRG CTR ARMAMENT ENGRG & TECHL CTR ATTN AMSRD AAR AEF T J MATT BLDG 305 APG MD 21005-5001	1 HC DIRECTOR US ARMY RSRCH LAB ATTN AMSRD ARL RO EV W D BACH PO BOX 12211 RESEARCH TRIANGLE PARK NC 27709
1 HC	US ARMY TRADOC BATTLE LAB INTEGRATION & TECHL DIRCRTT ATTN ATCD B 10 WHISTLER LANE FT MONROE VA 23651-5850	11 HC US ARMY RSRCH LAB ATTN AMSRD ARL CI OK T TECHL PUB (2 COPIES) ATTN AMSRD ARL CI OK TL TECHL LIB (2 COPIES) ATTN AMSRD ARL D J M MILLER ATTN AMSRD ARL SE RE D JUDY ATTN AMSRD ARL SE RL J PULSKAMP ATTN AMSRD ARL SE RL M DUBEY ATTN AMSRD ARL SE RL R POLCAWICH ATTN AMSRD ARL SE RM S WEISS ATTN IMNE ALC IMS MAIL & RECORDS MGMT ADELPHI MD 20783-1197
1 HC	PRODUCT MANAGER TIMS ATTN SFAE IEWS NS TIMS B GRIFFIES BLDG 563 FT MONMOUTH NJ 07703	TOTAL: 23 (1 elec, and 22 HCs)
1 HC	SMC/GPA 2420 VELA WAY STE 1866 EL SEGUNDO CA 90245-4659	
1 HC	US ARMY INFO SYS ENGRG CMND ATTN AMSEL IE TD F JENIA FT HUACHUCA AZ 85613-5300	